


# The Roles of Different Multigene Combinations of *Pdx1*, *Ngn3*, *Sox9*, *Pax4*, and *Nkx2.2* in the Reprogramming of Canine ADSCs Into IPCs

Cell Transplantation  
Volume 31: 1–11  
© The Author(s) 2022  
Article reuse guidelines:  
sagepub.com/journals-permissions  
DOI: 10.1177/09636897221081483  
journals.sagepub.com/home/ctj  


Dengke Gao<sup>1</sup>, Pengxiu Dai<sup>1</sup>, Zhixin Fan<sup>1</sup>, Jinglu Wang<sup>1</sup>, and Yihua Zhang<sup>1</sup>

## Abstract

Adipose-derived mesenchymal stem cells (ADSCs) are ideal sources for the treatment of diabetes, and the differentiation of ADSCs into insulin-producing cells (IPCs) through transfection of exogenous regulatory genes *in vitro* has been studied in depth. The differentiation of ADSCs is strictly regulated by a variety of transcription factors such as *Pdx1*, *Ngn3*, *Pax4*, *Nkx2.2*, and *Sox9*. However, whether these genes can coordinately regulate the differentiation of ADSCs into IPCs is still unknown. In this study, five multigene coexpressing adenovirus vectors (*pAdTrack-Pdx1-Ngn3-AdEasy*, *pAdTrack-Pdx1-Ngn3-Sox9-AdEasy*, *pAdTrack-Pdx1-Ngn3-Pax4-Sox9-AdEasy*, *pAdTrack-Pdx1-Ngn3-Nkx2.2-Sox9-AdEasy*, and *pAdTrack-Pdx1-Ngn3-Nkx2.2-Pax4-AdEasy*) were constructed, and then the stocks of the packaged adenoviruses were used to infect the canine ADSCs (cADSCs). Based on results of morphological observation, dithizone staining, sugar-stimulated insulin secretion test, cellular insulin immunofluorescence assays, and the detection of pancreatic  $\beta$ -cell development-related genes in the induced cells, the best induction combination (*pAdTrack-Pdx1-Ngn3-Nkx2.2-Pax4-AdEasy*) was identified after comparative screening. This study provides a theoretical reference and an experimental basis for further research on stem cell replacement therapy for diabetes.

## Keywords

adipose-derived mesenchymal stem cells (ADSCs), insulin-producing cells (IPCs), adenovirus, multigene coexpressing

## Introduction

Diabetes is one of the most common metabolic diseases in the world. In addition to disturbing people's daily life, diabetes occurs more often in dogs and cats. According to statistics, the incidence of diabetes in dogs and cats reaches about 0.4% to 1.2%, and the incidence of diabetes in dogs has reached 6% of the total number of clinical cases<sup>1,2</sup>. Traditional drug therapy and insulin injection therapy cannot treat diabetes dynamically and fundamentally<sup>3–5</sup>. Islet transplantation can effectively control blood glucose changes and avoid complications, but its clinical application is limited due to donor deficiency and immune rejection<sup>6</sup>. As reported, pluripotent stem cells can be induced to differentiate into cells with insulin-secreting function through targeted induction, which can provide a new method for the treatment of diabetes<sup>7,8</sup>. Adipose-derived mesenchymal stem cells (ADSCs) are ideal sources for the treatment of diabetes because they are derived from adipose tissue, easy to isolate and culture, and involve fewer medical ethical issues<sup>9</sup>.

Currently, the differentiation of ADSCs into insulin-producing cells (IPCs) *in vitro* has been studied in depth, and optimistic progress has been made<sup>10</sup>. In current research, transferring one to three exogenous regulatory genes cannot completely activate the cascade regulatory system of mesenchymal stem cells (MSCs) and is not sufficient to promote the differentiation of MSCs into pancreatic  $\beta$ -cells<sup>11–13</sup>. Moreover, this method needs to be greatly improved in terms of the induction efficiency, IPC maturity, and insulin secretion

<sup>1</sup> College of Veterinary Medicine, Northwest A&F University, Xianyang, China

Submitted: July 26, 2021. Revised: December 20, 2021. Accepted: February 2, 2022.

### Corresponding Author:

Yihua Zhang, College of Veterinary Medicine, Northwest A&F University, No. 3, Taicheng Road, Yangling District, Xianyang 712100, Shaanxi Province, China; Baioupai Tianjin Biotechnology Ltd., No.7 Juxing Road, Xianshuigu Town, Jinnan District, Tianjin 300350, China.  
Email: zyh19620207@163.com



**Table 1.** Primer Sequences of Genes With Different Homologous Fragments.

Genes	Sequences
<i>Pdx1</i> -UF	5'-gtcagatccgctagatctGCCACCATGAACAGCGAGGAACAGTTCT-3'
<i>Pdx1</i> -UR	5'-aggatgaggggcatAGGTCCGGGGTTAGATTCACG-3'
<i>Ngn3</i> -UF	5'-tctaaccgggacctGCCACCATGGCCCCTCATCCTTCTGGTG-3'
<i>Ngn3</i> -AR	5'-gatatcttctagaagctTCACAGGAAATCAGAGAAGGCC-3'
<i>Ngn3</i> -BR	5'-gtccagcaggttcatAGGTCCGGGGTTCTCTTCCACG-3'
<i>Ngn3</i> -CR	5'-tccgacttgaggcatAGGTCCGGGGTTCTCTTCCACG-3'
<i>Ngn3</i> -DR/ER	5'-gttggtcaggtcatAGGTCCGGGGTTCTCTTCCACG-3'
<i>Sox9</i> -BF	5'-gagaacccggacctGCCACCATGAACCTGCTGGACCCGTTCA-3'
<i>Sox9</i> -CF	5'-agcaacccggacctGCCACCATGAACCTGCTGGACCCGTTCA-3'
<i>Sox9</i> -DF	5'-gagaaccctggacctGCCACCATGAACCTGCTGGACCCGTTCA-3v
<i>Sox9</i> -UR	5'-gatatcttctagaagctTCAGGGTCTTGTCAGTGGGGTG-3'
<i>Pax4</i> -CF	5'-gagaacccggacctGCCACCATGCCTCAAGTCGGATGGGGCG-3'
<i>Pax4</i> -CR	5'-gtccagcaggttcatAGGTCCGGGGTTGCTTCCACG-3'
<i>Pax4</i> -EF	5'-gagaaccctggacctGCCACCATGCCTCAAGTCGGATGGGGCG-3'
<i>Pax4</i> -ER	5'-gatatcttctagaagctTCAGCCGATTTCTTTGCCGGCC-3'
<i>Nkx2.2</i> -DF/EF	5'-gagaacccggacctGCCACCATGAGCCTGACCAACACCAAGA-3'
<i>Nkx2.2</i> -DR	5'-gtccagcaggttcatAGGTCCAGGGTTCTCTTCCACG-3'
<i>Nkx2.2</i> -ER	5'-tccgacttgaggcatAGGTCCAGGGTTCTCTTCCACG-3'

The small font portion of the primer is the overlapping area. F and R represent the forward primers and reverse primers, respectively. U represents universal for all combinations.

A: combination A (*Pdx1*+*Ngn3*); B: combination B (*Pdx1*+*Ngn3*+*Sox9*); C: combination C (*Pdx1*+*Ngn3*+*Pax4*+*Sox9*); D: combination D (*Pdx1*+*Ngn3*+*Nkx2.2*+*Sox9*); E: combination E (*Pdx1*+*Ngn3*+*Nkx2.2*+*Pax4*).

level. Therefore, screening and optimizing a high-efficiency regulatory gene combination, which can reprogram ADSC differentiation into cells that are sensitive to changes in sugar concentration and whose insulin content and release are comparable to normal pancreatic  $\beta$ -cells, are of great significance for the study of cell transplantation treatment in diabetes.

The differentiation of ADSCs is strictly regulated by a variety of transcription factors. For example, *Pdx1* can activate the regulation of early embryonic pancreatic development<sup>14</sup>, *Ngn3* can initiate the differentiation of pancreatic precursor cells into pancreatic endocrine cells<sup>15</sup>, *Pax4* plays an important regulatory role in the production of islet progenitor cells and the differentiation of islet  $\beta$ -cells<sup>16</sup>, and *Nkx2.2* is necessary for the phenotypic determination of mature  $\beta$ -cells<sup>17</sup>. A large number of studies have confirmed that transfection of *Pdx1*, *Ngn3*, *Pax4*, or *Nkx2.2* into stem cells can induce their differentiation into IPCs<sup>18–20</sup>. A *Pdx1*-*Ngn3* combined transfection can mediate the reprogramming of mesenchymal stromal cell differentiation into pancreatic endocrine cells *in vitro*<sup>12</sup>. In a previous study, we also confirmed that *Sox9* can promote the differentiation of canine ADSCs (cADSCs) into islet-like cells. However, whether *Pax4*, *NKX2.2*, and *Sox9* can coordinate with *Pdx1*-*Ngn3* to regulate the reprogramming process of ADSC differentiation into islet cells is still unknown.

Therefore, in this study, five multigene coexpressing adenovirus vectors based on *Pdx1*-*Ngn3*, *Pax4*, *Nkx2.2*, and *Sox9* were constructed, and the stocks of the packaged adenoviruses were used to infect the cADSCs, respectively. By detecting the differentiation effects of the five multigene

adenoviruses on ADSCs, the best inducing gene combination was determined to provide a theoretical and experimental basis for further research on stem cell replacement therapy for diabetes.

## Materials and Methods

### Amplification of *Pdx1*, *Ngn3*, *Sox9*, *Pax4*, and *Nkx2.2* Genes

The coding sequences of *Pdx1* (GeneID: 493994), *Ngn3* (GeneID: 489022), *Sox9* (GeneID: 403464), *Pax4* (GeneID: 482268), and *Nkx2.2* (GeneID: 485744) were synthesized by Wuhan GeneCreate Biological Engineering Company. In addition, the end of each gene was connected to different 2A sequences (*Pdx1*+*E2A*; *Ngn3*+*P2A*; *Sox9*+*P2A*; *Pax4*+*E2A*; *Nkx2.2*+*T2A*) and cloned into pUC57. Primers with homologous fragments were designed according to the target gene sequences of the different gene combinations (A: *Pdx1*+*Ngn3*; B: *Pdx1*+*Ngn3*+*Sox9*; C: *Pdx1*+*Ngn3*+*Pax4*+*Sox9*; D: *Pdx1*+*Ngn3*+*Nkx2.2*+*Sox9*; E: *Pdx1*+*Ngn3*+*Nkx2.2*+*Pax4*; Supplementary Fig. 1B) and the *pAdTrack-CMV* vector (Hunan Fenghui Biotechnology Company, Hunan, China) sequences (Table 1) (which contains *GFP* gene sequences, and the plasmid map can be found in Supplementary Fig. 1A). There was an overlap region of approximately 20 bp between the forward primer of the first gene of each combination and the *Bgl* II sites of *pAdTrack-CMV*, and there was an overlap region of approximately 15 bp

**Table 2.** Primer Sequences of the Recombinant Genes.

Genes	Sequences
<i>PAD-Pdx1-F</i>	5'-CCACTTGGCAGTACATCA-3'
<i>PAD-Pdx1-R</i>	5'-CGGTCAGATTCAGCATCA-3'
<i>Pdx1-Ngn3-F</i>	5'-TTACGAAAGTGCCTCCTCT-3'
<i>Pdx1-Ngn3-R</i>	5'-GCCTCTTCTTGTCTCAGT-3'
<i>Ngn3-PAD-F</i>	5'-AAGAAGGCGGAGGTTGTA-3'
<i>Ngn3-PAD-R</i>	5'-TCACTAGCAGATCGTCGAT-3'
<i>Ngn3-Sox9-F</i>	5'-AAGAAGGCGGAGGTTGTA-3'
<i>Ngn3-Sox9-R</i>	5'-GTGGTTGGAGGTGTAGGA-3'
<i>Sox9-PAD-F</i>	5'-GAACGAGAGCGAGAAGAG-3'
<i>Sox9-PAD-R</i>	5'-TGTGGTATGGCTGATTATGA-3'
<i>Ngn3-Pax4-F</i>	5'-AAGAAGGCGGAGGTTGTA-3'
<i>Ngn3-Pax4-R</i>	5'-TAGGTTGAGGAGGCAGATAT-3'
<i>Pax4-Sox9-F</i>	5'-CAGTCAGAGTGTGGTTCAG-3'
<i>Pax4-Sox9-R</i>	5'-GTGGTTGGAGGTGTAGGA-3'
<i>Ngn3-Nkx2.2-F</i>	5'-TCCTTCTGGTGCTCCTAC-3'
<i>Ngn3-Nkx2.2-R</i>	5'-GTA'TCTCTGCTGCCTGAAC-3'
<i>Nkx2.2-Sox9-F</i>	5'-GACAAGGTGCTCTGGATG-3'
<i>Nkx2.2-Sox9-R</i>	5'-GTGGTTGGAGGTGTAGGA-3'
<i>Nkx2.2-Pax4-F</i>	5'-GACAAGGTGCTCTGGATG-3'
<i>Nkx2.2-Pax4-R</i>	5'-TTGCTGAACCACACTCTG-3'
<i>Pax4-PAD-F</i>	5'-GCAAGAGGACCAGAGACT-3'
<i>Pax4-PAD-R</i>	5'-GGACAAACCACAACACTAGAATG-3'

between the forward and reverse primers of the connected genes. The reverse primer of the last gene had an overlap region of 20 bp with the *Hind* III sites of *pAdTrack-CMV*. The target gene fragment was amplified by polymerase chain reaction (PCR) and confirmed by DNA sequencing.

### Construction of Multigene Coexpression Adenovirus Vectors

The *pAdTrack-CMV* was digested with *Bgl* II and *Hind* III (TaKaRa, Dalian, China) to obtain a linearized vector. The *Pdx1*, *Ngn3*, *Sox9*, *Pax4*, and *Nkx2.2* gene fragments were connected to the linearized vector in the order of each combination according to the instructions of the EasyGeno Rapid Recombination Cloning Kit (Beijing Tian Gen Biotechnology Company, Beijing, China) (Supplementary Fig. 1). The different constructed adenovirus shuttle vectors were verified by segmented PCR (see Table 2 for primer information) and double enzyme digestion experiments.

The correctly identified shuttle vectors were linearized by *Pme* I (New England Biolabs, MA, USA) enzyme digestion and then transferred to BJ5183-AD-1 competent cells (containing pAdeasy-1) for recombination. These obtained adenovirus backbone vectors were identified by *Pac* I (New England Biolabs) restriction enzyme digestion. Using the Advanced Transfection Reagent kit (Zeta Life, San Francisco, CA, USA), the constructed vectors were transfected into 293A cells for adenovirus packaging to obtain infectious multigene coexpression adenovirus stocks.

### Canine ADSC Culture

The cADSCs were isolated and identified by the Shaanxi Stem Cell Engineering Technology Research Center<sup>21</sup>. The cryopreserved cADSCs were resuscitated with  $\alpha$ -MEM medium and cultured in a 37°C, 5% CO<sub>2</sub> incubator. When the cell confluency reached approximately 60%, the successfully constructed multigene adenovirus stock was added to the cells at an MOI (multiplicity of infection) of 100 and then cultured further.

### Reverse transcription quantitative PCR

The total RNA was extracted with the TaKaRa MiniBEST Universal RNA Extraction Kit (Code No. 9767). The total RNA was then reverse transcribed into complementary DNA (cDNA) according to the Takara PrimeScript<sup>TM</sup>RT Master Mix (Perfect Real Time) (Code No. RR036Q) instructions. cDNA was used as a template to detect the expression of the target gene by quantitative PCR (qPCR), based on the primers listed in Table 3. The *GAPDH* gene was used as an internal control. The specific measured methods were carried out as previously described<sup>22</sup>. The verification was repeated three times for each gene of each sample, and the gene expression level was quantified using the 2<sup>- $\Delta\Delta$ Ct</sup> method<sup>23</sup>.

### Western Blot

A total of 50  $\mu$ g protein was separated by sodium dodecyl sulfate (SDS)-polyacrylamide gel electrophoresis (PAGE) as previously described<sup>24</sup>. Primary antibodies against the targeted proteins included an anti-beta-actin antibody (ab8227, 1:2,000; Abcam, Cambridge, UK), anti-PDX1 antibody (ab227586, 1:1,000; Abcam), anti-NGN3 antibody (ab176124, 1:1,000; Abcam), anti-NKX2.2 antibody (ab86024, 1:1,000; Abcam), anti-PAX4 antibody (ab101721, 1:1,000; Abcam), and anti-SOX9 antibody (ab26414, 1:1,000; Abcam).

### Dithizone Staining

Dithizone staining was performed according to a previously published method<sup>25</sup>. The cells were stained for 15 min with a freshly prepared dithizone (Sigma-Aldrich, MO, USA) working solution at 37°C, and observed and photographed under an optical microscope.

### Glucose-Stimulated Insulin Secretion

A low-glycemic serum-free Dulbecco's Modified Eagle Medium (DMEM) (containing 5.6 mmol/l glucose), a high-glycemic serum-free DMEM (containing 25 mmol/l glucose), or a KCl stimulation solution (containing 30 mmol/l KCl) was added to the cells for incubation for 30 min. After that, the canine Insulin Quantikine ELISA Kit (DINS00) was used to detect insulin secretion in the cell supernatant or cell

**Table 3.** Primer Sequences Used for Real-Time PCR.

Genes	Sequences
<i>Pdx1-Exogenous-F</i>	5'-CAACTGCTGGAAGTGGAA-3'
<i>Pdx1-Exogenous-R</i>	5'-CGCTTCTTGTCTCTTCTT-3'
<i>Ngn3-Exogenous-F</i>	5'-AGCGGAGAAGCAGAAGAA-3'
<i>Ngn3-Exogenous-R</i>	5'-ATGTAGTTGTGGGCGAATC-3'
<i>Pax4-Exogenous-F</i>	5'-TGGCGGAGACAAGAGAAG-3'
<i>Pax4-Exogenous-R</i>	5'-GCACAGATCCTGGAGACT-3'
<i>Nkx2.2-Exogenous-F</i>	5'-TCAGGCAGCAGAGATACC-3'
<i>Nkx2.2-Exogenous-R</i>	5'-TTCTAGGAGATGGCAGAGG-3'
<i>Sox9-Exogenous-F</i>	5'-ACGGACAAGTGACCTACA-3'
<i>Sox9-Exogenous-R</i>	5'-GAGGAGCCTGTGGAGATT-3'
<i>GAPDH-F</i>	5'-GCTGAGTATGTTGTGGAGT-3'
<i>GAPDH-R</i>	5'-GCAGAAGGAGCAGAGATG-3'
<i>Pdx1-F</i>	5'-GTGGATGAAGTCTACCAAGG-3'
<i>Pdx1-R</i>	5'-TTGAACAGGAACTCCTTCTC-3'
<i>Pax4-F</i>	5'-GGAGACATCACCAGACAG-3'
<i>Pax4-R</i>	5'-AATGGAGGCAATGGAAGG-3'
<i>Gata4-F</i>	5'-CAGCAACTCCAGCAATGT-3'
<i>Gata4-R</i>	5'-ATCGCACTGACTGAGAATG-3'
<i>Nkx2.2-F</i>	5'-CTTCTCCAAGGCACAGAC-3'
<i>Nkx2.2-R</i>	5'-TCTTGTAGCGGTGGTTCT-3'
<i>Nkx6.1-F</i>	5'-GGAGAGTCAGGTCAAGGT-3'
<i>Nkx6.1-R</i>	5'-GTTGTAGTCGTCGTCCTC-3'
<i>MafA-F</i>	5'-AGCAAGGAGGAGGTCATC-3'
<i>MafA-R</i>	5'-CTTCTCGCTCTCCAGGAT-3'
<i>SLC30A8-F</i>	5'-CAGAGCCACCAAGATGTAT-3'
<i>SLC30A8-R</i>	5'-CCGAAGCAGCATAGAGTT-3'
<i>ABCC8-F</i>	5'-GCTGTGCTTCTCTTCCCT-3'
<i>ABCC8-R</i>	5'-GGTCTGTATTGCTCCTCTC-3'
<i>KCNJ8-F</i>	5'-CTCGCCAACCAAGACCTA-3'
<i>KCNJ8-R</i>	5'-CCTCCTCCTCAGTTACAATAG-3'
<i>G6PC2-F</i>	5'-CCAGAGTATTCATAGCAACAC-3'
<i>G6PC2-R</i>	5'-GGTCAATGTCAAGCAGTCT-3'
<i>PCSK1-F</i>	5'-AGTGGAGAAGATGGTGGAT-3'
<i>PCSK1-R</i>	5'-TTGTAGGAGTCTAAGCAATG-3'
<i>PCSK2-F</i>	5'-TATGACTTTCAGCGGCAAT-3'
<i>PCSK2-R</i>	5'-GCGACCTTGGAGTTGTAT-3'
<i>Insulin-F</i>	5'-GCTTCTTCTACACGCCTAA-3'
<i>Insulin-R</i>	5'-CTAGTTGCAGTAATTCTCCAG-3'

culture fluid, and then normalized by cell count. The insulin stimulation release index, SI, is the ratio of insulin secretion after high-glucose stimulation to that after low-glucose stimulation.

### Immunofluorescence Assay

The immunofluorescence staining was performed according to a previously published method<sup>25,26</sup>. The cells were fixed in 4% paraformaldehyde for 20 to 30 min, triple-washed with phosphate-buffered saline (PBS), stained with rabbit antibodies against dog insulin (ab63820, 1:100; Abcam), and then stained with DyLight594-labeled goat anti-rabbit IgG secondary fluorescent antibodies (35560, 1:100;

Invitrogen, Carlsbad, CA, USA). In addition, Hoechst 33342 (Beijing Solarbio Science & Technology Company, Beijing, China) was used to counterstain the cell nuclei, after which the cells were photographed with an inverted fluorescence microscope.

### Statistical Analysis

Statistical analysis was performed using SPSS 20.0. A one-way analysis of variance or *t* test was used to assess the difference between the two groups or between multiple groups. A value of  $P < 0.05$  was considered statistically significant.

## Results

### Identification and Packaging of Multigene Coexpression Adenovirus Vectors

First, we cloned specific gene fragments that contain different homology arms (A: *Pdx1-Ngn3*; B: *Pdx1-Ngn3-Sox9*; C: *Pdx1-Ngn3-Pax4-Sox9*; D: *Pdx1-Ngn3-Nkx2.2-Sox9*, and E: *Pdx1-Ngn3-Nkx2.2-Pax4*) from pUC57 plasmids (Supplementary Fig. 2) and then reconnected these fragments with the vector *pAdTrack-CMV* that was digested by *Bgl* II and *Hind* III to obtain different adenovirus shuttle vectors. The obtained vectors were verified by segmented PCR and double enzyme digestion (*Bgl* II and *Hind* III), and the electrophoresis results showed that all vectors were consistent with the expected product size (Supplementary Figs. 3 and 4A), which proved that the five groups of adenovirus shuttle vectors were successfully constructed.

Afterward, the five groups of adenovirus shuttle vectors, treated with *Pme* I enzyme, were transferred into BJ5183-AD-1 competent cells to obtain different adenovirus backbone vectors. These obtained adenovirus backbone vectors were processed by the restriction endonuclease *Pac* I for reverse verification, and the electrophoresis results showed that two bands of approximately 30 kb and 5 kb were consistent with the expected product sizes (Supplementary Fig. 4B).

Then the adenovirus backbone vectors treated with *Pac* I enzyme were purified, recovered, and then transfected into 293A cells, respectively. A small amount of green fluorescence was observed in the cells after 24 h of culture, and green fluorescence was seen in the cells in the full field view after 48 h (Supplementary Fig. 4C). When the cells were continuously cultured until they were observed to be in the shape of grape clusters, we collected the cell suspension and performed repeated freezing and thawing to collect the successfully packaged A, B, C, D, and E combination adenovirus stocks.

### Expression of Exogenous Genes in cADSCs After Infection With Multigene Adenovirus Stocks

We used the successfully constructed adenovirus stocks of the five combinations of A, B, C, D, and E to infect the cADSCs, respectively, and then assess the expression levels of

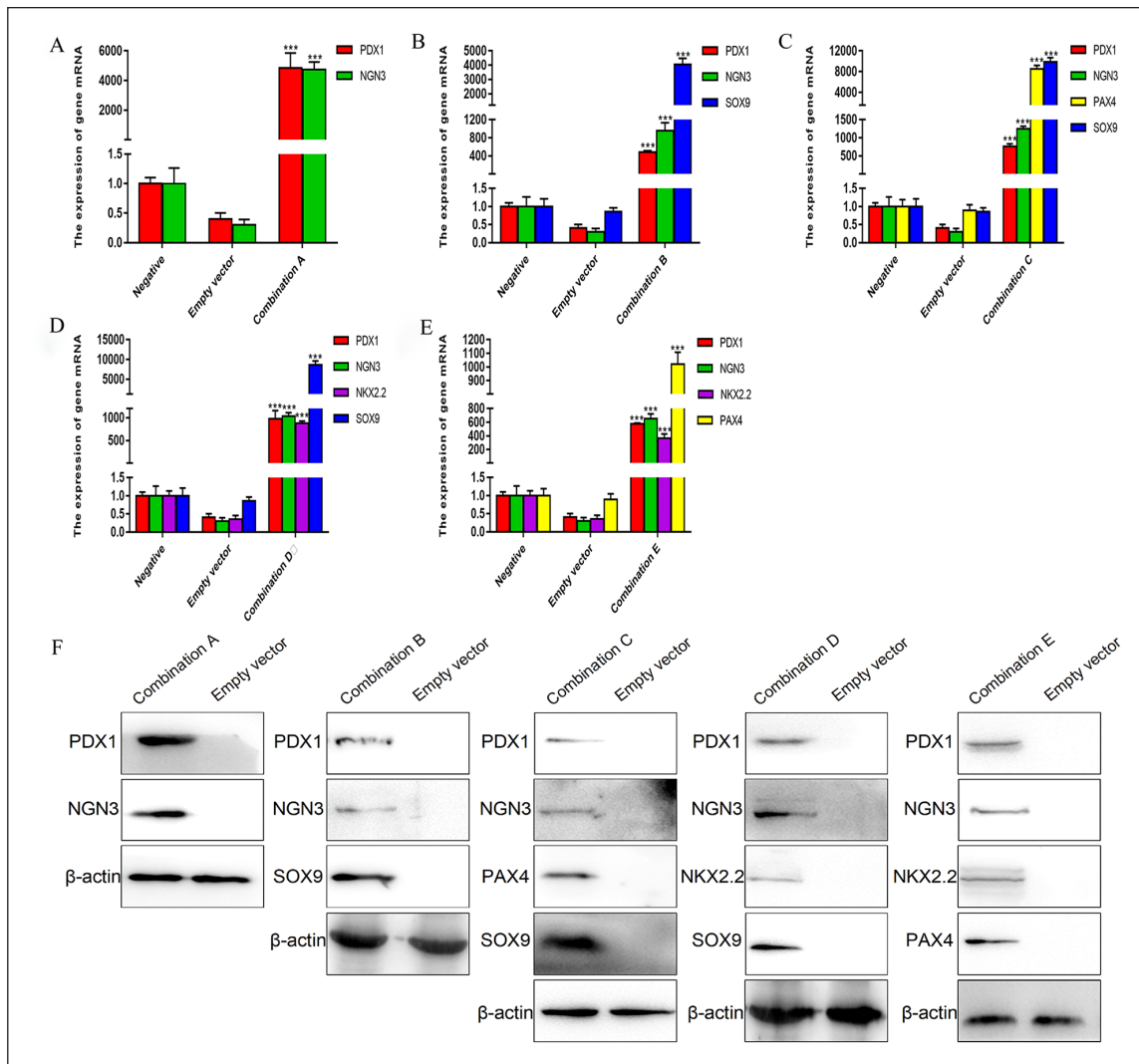


**Figure 1.** The expression levels of exogenous genes in cADSCs after infection with multigene adenovirus stocks. (A–E) The mRNA expression levels of exogenous genes in cADSCs after infection with the five multigene adenovirus stocks; (F) the protein expression levels of exogenous genes in cADSCs after infection with the five multigene adenovirus stocks. cADSCs: canine adipose-derived mesenchymal stem cells; mRNA: messenger RNA. \*\*\* $P < 0.001$  versus the negative group.

the exogenous genes in the cADSCs after 4 days of culture. The results from the reverse transcription quantitative (RT-qPCR) and western blotting showed that the expression of the corresponding exogenous transfected gene in the cells after infection was significantly higher than that of the control group, and the trends of the messenger RNA (mRNA) level and the protein level of the target gene were roughly the same (Fig. 1). The results indicated that these five combinations of adenoviruses can successfully introduce different exogenous genes into cADSCs.

### Expression of GFP in cADSCs After Infection With Multigene Adenovirus Stocks

To understand the effect of the multigene coexpressing adenoviruses on cADSCs, we observed the cell morphology and

green fluorescent protein (GFP) expression in cADSCs during the infection process by microscopic evaluation (Fig. 2). A large amount of relatively weak GFP expression was detected in the cADSCs infected with the five combination adenoviruses after 2 days. The fluorescence intensity of GFP in the cells infected by each combination of adenovirus increased significantly after 4 days of infection. At the end of the 30-day induction, the adenovirus-infected cells in each group appeared clustered and showed a spherical shape of pancreatic islet-like cells. However, the empty vector-infected cells did not clump by the 30th day, and their GFP expression decreased significantly.

After induction for 30 days, the number of cell agglomerates in the combinations of A, B, C, D, and E were significantly higher than those of the empty control group (Fig. 3). For example, there were approximately 103 cell clusters in

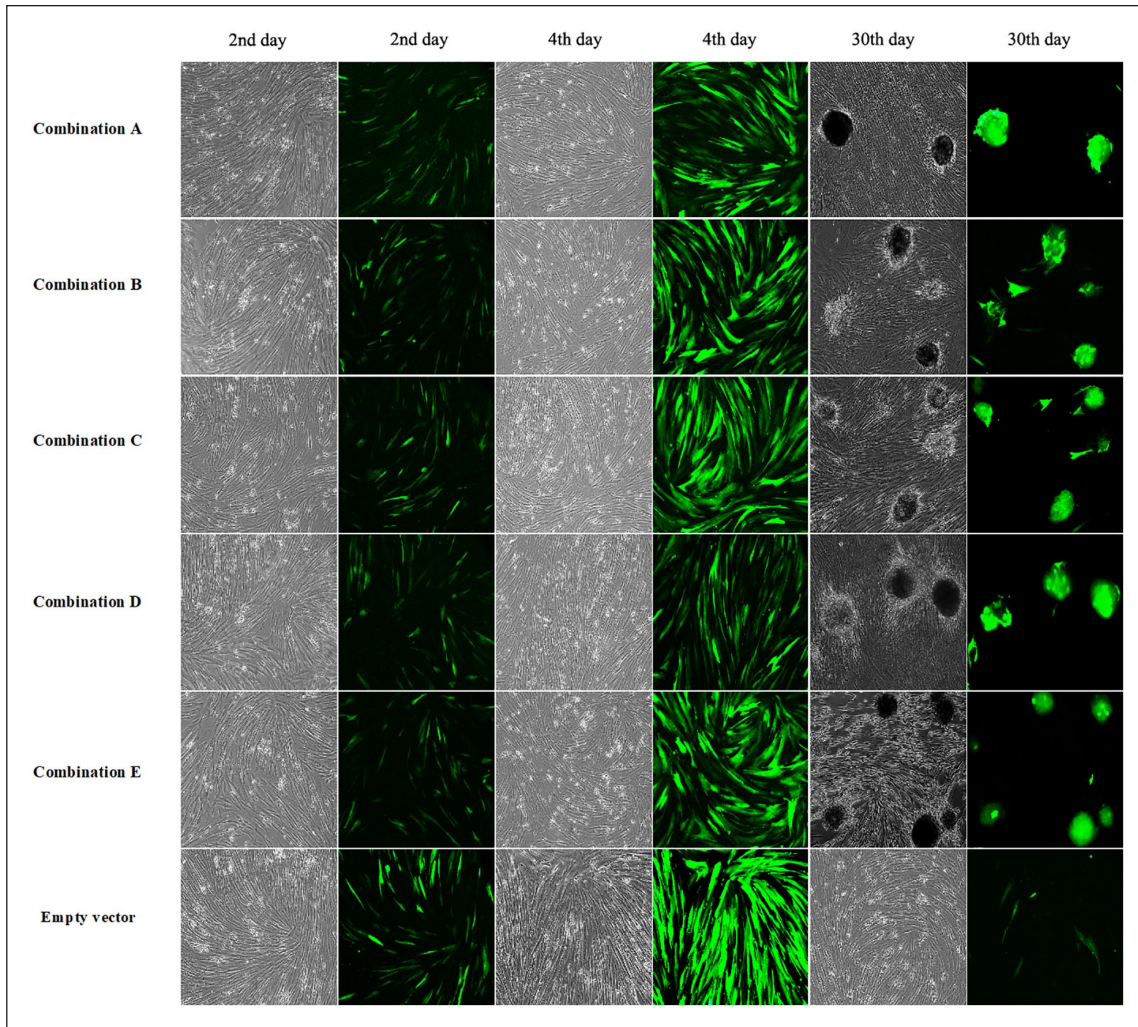


**Figure 2.** The cell morphology change (bright field) and green fluorescent protein expression (fluorescent images) in canine adipose-derived mesenchymal stem cells after infection with multigene adenovirus stocks ( $100\times$  magnification) on the 2nd, 4th, and 30th day.

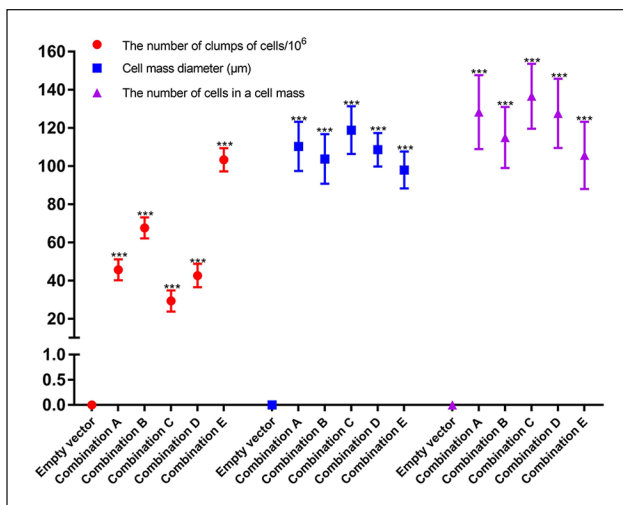


**Figure 3.** Statistical analysis of the cell agglomerates after infection with multigene adenovirus stocks for 30 days. \*\*\* $P < 0.001$  versus the empty vector control group.

$10^6$  cADSC cells, the diameter of the cell cluster was approximately  $98 \mu\text{m}$ , and each cell cluster contained approximately 105 cells in group E. This phenomenon of cell clustering indicates that the cells had a preference to differentiate into pancreatic islet-like cell clusters.

#### Identification of Islet-Like Cell Clusters After Infection of cADSCs With Multigene Adenovirus Stocks

We used dithizone staining to identify whether the cADSC cell group induced by multigene coexpression adenovirus infection had the characteristics of islet-like cells. The cell clusters after induction for 30 days with A, B, C, D, or E combinations all showed scarlet red staining after dithizone staining, while the cells in the empty vector control group did not show scarlet staining (Fig. 4). This result indicated that the cell clusters induced by multigene coexpression adenovirus infection exhibited the characteristics of islet cells.

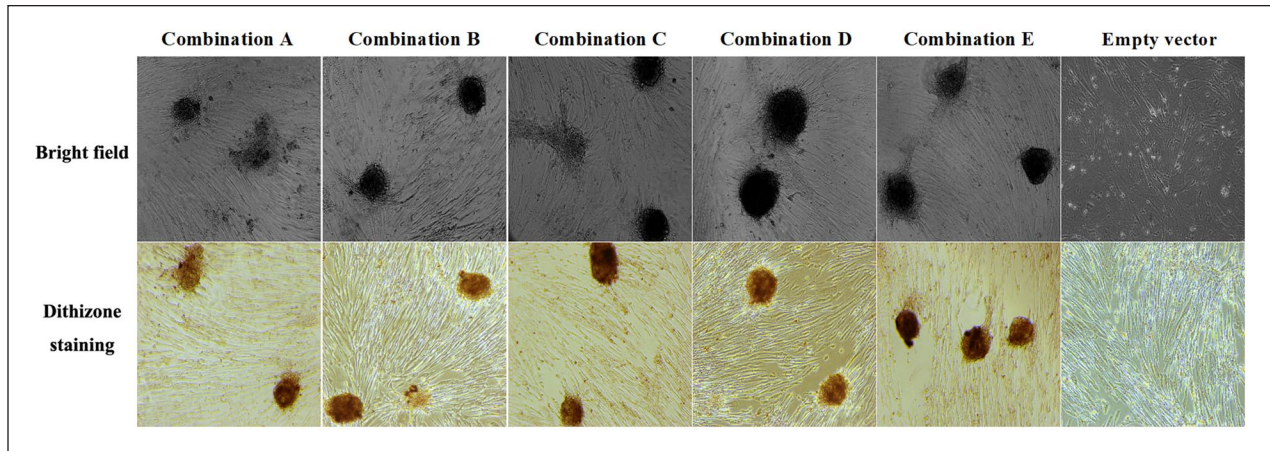


**Figure 4.** Dithizone staining of canine adipose-derived mesenchymal stem cells after infection with multigene adenovirus stocks (100 $\times$  magnification).

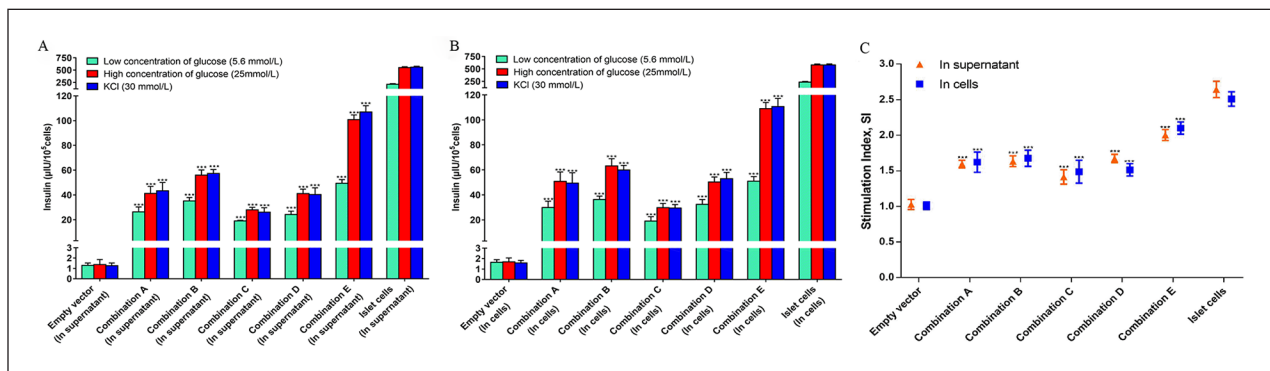


**Figure 5.** Insulin secretion and insulin stimulation release index of canine adipose-derived mesenchymal stem cells after infection with multigene adenovirus stocks. (A) Insulin secretion in the supernatants; (B) insulin secretion into the cell culture fluid; (C) insulin stimulation release index.  $***P < 0.001$  versus the empty vector control group.

### Insulin Secretion of cADSCs After Infection With Multigene Adenovirus Stocks

To further determine whether the cell clusters that were induced by the infection of the different multigene coexpression adenoviruses had the function to produce insulin, we performed glucose stimulation tests on canine pancreatic islet cells and the cells that were infected with adenoviruses with different combinations of multigene (Fig. 5). The results of insulin secretion in the cell supernatant and cell fluid showed that the insulin contents of the cells of five groups were significantly higher than those of the empty vector group but lower than those of the islet cells (Fig. 5A, B). The insulin secretion measured in the cell fluid was slightly higher than that of the supernatant, and the insulin secretion levels after KCl stimulation and high-glucose stimulation were similar. The insulin secretion of the E group cells was the largest among the five induction groups, and the insulin stimulation release index SI of the E group cells (SI in the supernatant was 2.00; SI in the cell fluid was 2.10) was also

higher than that of the cells of other four groups but lower than that of the islet cells (SI in the supernatant was 2.65; SI in the cell fluid was 2.51) (Fig. 5C).

In addition, the insulin immunofluorescence results of the cells after infection with the five groups of multigene adenovirus stocks all showed the red fluorescence (Fig. 6). However, only blue-stained nuclei were observed in the cells infected with the empty vector. The result confirmed that infection of the cADSCs with the five multigene coexpressing adenoviruses could induce the production of IPCs.

### The Expression of Genes Related to the Development of Islet $\beta$ -Cells After Infection of cADSCs With Multigene Adenovirus Stocks

To understand the regulation process of cADSC differentiation into islet-like cells induced by different multigene adenoviruses, we tested the expression levels of pancreatic  $\beta$ -cell development-related genes (*Pdx1*, *Pax4*, *Gata4*, and

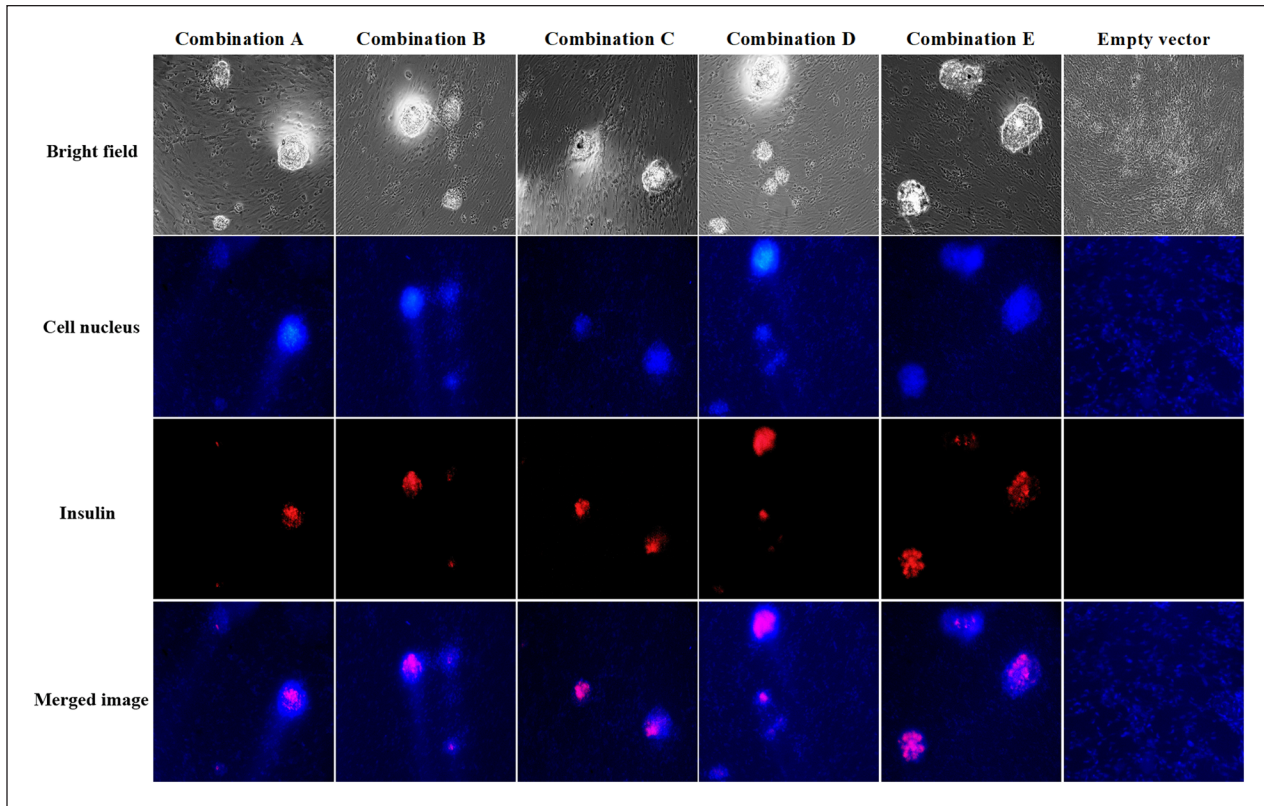


**Figure 6.** Insulin immunofluorescence staining of canine adipose-derived mesenchymal stem cells after infection with multigene adenovirus stocks (100 $\times$  magnification).

*Nkx2.2*), insulin secretion-related genes (*Nkx6.1*, *MafA*, *SLC30A8*, *ABCC8*, *KCNJ8*, and *G6PC2*), and insulin formation-related genes (*PCSK1*, *PCSK2*, and *Insulin*) in the differentiated cells. As shown in Fig. 7, the expression levels of islet  $\beta$ -cell development-related genes (*Pax4* and *Nkx2.2*), insulin secretion-related genes (*Nkx6.1*, *ABCC8*, and *KCNJ8*), and insulin formation-related genes (*PCSK1*, *PCSK2*, and *Insulin*) in the cells infected with the five multigene coexpressing adenoviruses were significantly higher than in the cells of the empty vector group. Among them, the gene expression levels of *Insulin*, *PCSK2*, and *SLC30A8* of groups B and E were significantly higher than those of groups A, C, and D, and the gene expression of group E was higher than that of group B. These results indicate that the E group infection had the highest efficiency in inducing cADSCs to differentiate into pancreatic islet cells. When compared with the pancreatic islet cell group, the expression levels of *Pdx1*, *MafA*, *Nkx2.2*, *Pax4*, *Gata4*, *Insulin*, and *ABCC8* were still lower in group E.

## Discussion

ADSCs contain biologically active substances that regulate blood sugar balance, such as leptin, adipocytokines, and visfatin, and are better sources of seed cells for diabetes cell transplantation therapy compared with other MSCs<sup>27,28</sup>.

Many studies have reported that transferring key genes that regulate the development of islet  $\beta$ -cells into ADSCs can induce them to differentiate into IPCs<sup>18,29,30</sup>. However, only part of the cascade-regulated gene expression can be found in the induced IPCs, and the ability to secrete insulin from IPCs is limited. The main reason may be that the screening of exogenous regulatory genes has not been sufficiently comprehensive. Currently, many researchers often simultaneously overexpress multiple foreign genes in a target cell to study their mutual synergy or inhibition. Previous studies have reported that the combined induction of multiple different exogenous genes can promote the differentiation of MSCs into IPCs with insulin secretion function, and the induction effect of multiple genes was significantly better than that of induction with a single gene<sup>12</sup>.

In this study, we used the 2A sequence to carry out the recombination connection between multiple foreign genes<sup>31</sup>. Adenovirus vector-mediated gene transfer has the advantages of instantaneous high-level transgene expression and nonintegration into chromosomes<sup>32</sup>. Therefore, we had successfully constructed five multigene coexpression adenovirus vectors using this ideal transgenic tool. We tested the expression of exogenous genes after infection of cADSCs with these adenovirus stocks. It was found that the expression levels of the exogenous genes in the cells after infection with the five multigene adenoviruses were significantly



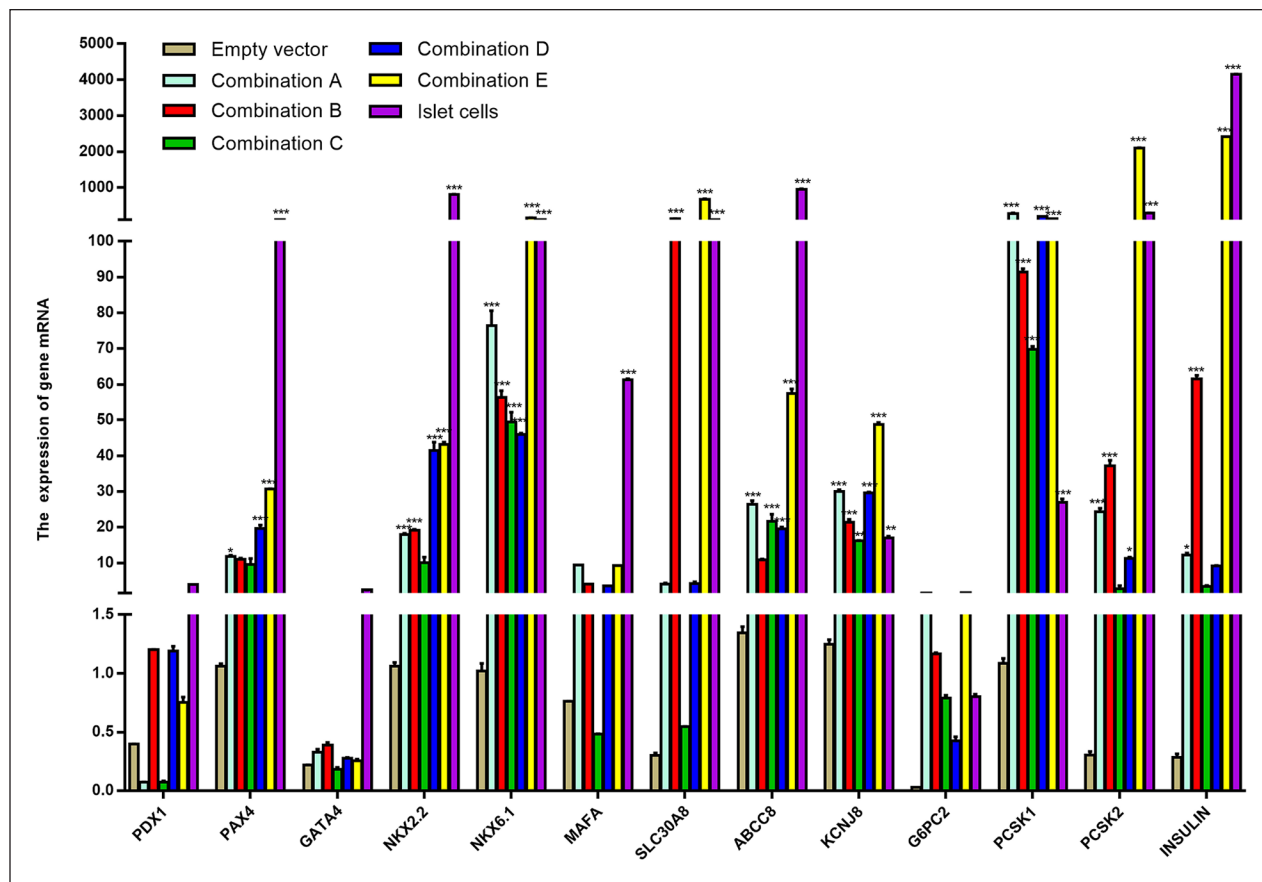


**Figure 7.** The mRNA expression levels of islet  $\beta$ -cell development-related genes of canine adipose-derived mesenchymal stem cells after infection with multigene adenovirus stocks. \* $P < 0.05$ , \*\* $P < 0.01$ , \*\*\* $P < 0.001$  versus the empty vector control group. mRNA, messenger RNA.

higher than those of the control group, and the expression levels of exogenous genes in the different multigene groups were also significantly different. As previous studies have reported, there are many factors, such as size, location, number, and type of the target gene, that can affect the final gene expression in the infected cells in 2A peptide-mediated coexpression of multiple genes<sup>33</sup>. We used different 2A peptides to connect multiple genes, and as the cleavage efficiencies of the different 2A peptides are different, this might cause more uncertainty in the cleavage efficiency<sup>34</sup>. Thus, this result may be due to the connection sequence of the different genes and the different cutting efficiency of the 2A peptide when we constructed the vectors. Interestingly, the results of RT-qPCR and western blotting revealed that the expression levels of the last gene in multiple combinations were higher than those of the other genes, and the specific reasons for this phenomenon still need to be further explored.

Cell differentiation is affected by both the combination of gene control programs and the microenvironment where the cell is located. Among these, genetic programming is the decisive factor that controls the differentiation of stem cells, and the external environment can only play a role by

influencing the selective expression of genetic programming within the cell. To study the genetic control program for the differentiation of ADSCs into pancreatic  $\beta$ -cells, we infected cADSCs with the adenovirus stocks of A, B, C, D and E combinations and then tested the induction effect of each combination. At first, we found that cells in all five groups showed pancreatic islet-like cell clusters after induction with the five polygenic adenoviruses, and the cell immunofluorescence results were positive for dithizone and insulin staining. However, by comparing the amount of insulin secretion, SI, and the mRNA expression of islet development-related genes, we found that the E combination (*pAdTrack-Pdx1-Ngn3-Nkx2.2-Pax4-AdEasy*) had the best induction effect, and the induction effect of the B combination (*pAdTrack-Pdx1-Ngn3-Sox9-AdEasy*) was better than that of the A (*pAdTrack-Pdx1-Ngn3-AdEasy*), C (*pAdTrack-Pdx1-Ngn3-Pax4-Sox9-AdEasy*) and D (*pAdTrack-Pdx1-Ngn3-Nkx2.2-Sox9-AdEasy*) combinations. These findings indicate that the coordinated expression of *Pdx1*, *Ngn3*, *Nkx2.2*, and *Pax4* plays an important role in the gene control program that induces the differentiation of cADSCs into IPCs. At the same time, it also showed that *Sox9* had a synergistic effect with

*Pdx1* and *Ngn3*, but when *Nkx2.2* or *Pax4* was added to the three-gene combination (*Pdx1-Ngn3-Sox9*), antagonism may have occurred and led to poor induction effects. The specific reason needs to be further experimentally studied. In addition, although the exogenous genes *Pdx1*, *Ngn3*, *Pax4*, *Nkx2.2*, and *Sox9* were successfully introduced into cADSCs in the form of different combinations and induced cADSCs to differentiate into IPCs, the insulin secretion level of cells that were infected with the adenovirus carrying the best gene combination of *Pdx1-Ngn3-Nkx2.2-Pax4* was still extremely significantly lower than that of the islet cells, which is far from the goal of a clinical diabetes treatment.

The same transcription factor exhibits different effects at different developmental stages in the pancreas, and the *in vivo* microenvironment can facilitate further induction and maturation of pancreatic  $\beta$ -cells to compensate for the damaged pancreatic  $\beta$ -cells and regulate blood sugar levels<sup>35,36</sup>. Therefore, in the follow-up research, we will further optimize the induction program by adding exogenous activin<sup>37</sup>, controlling the time point of gene expression<sup>38</sup>, creating a cell microenvironment, and ultimately screening different combinations of transgene induction.

## Conclusion

In this study, five groups of multigene coexpressing adenoviruses were used to infect cADSCs to induce them to differentiate into IPCs. Through morphological observation, dithizone staining, sugar-stimulated insulin secretion test, cellular immunofluorescence, and RT-qPCR assessment in the induced cells, the best induction combination (*pAdTrack-Pdx1-Ngn3-Nkx2.2-Pax4-AdEasy*) was identified after comparative screening. This study provides a theoretical reference and an experimental basis for further exploration of more efficient diabetic cell transplantation programs.

## Author's Note

Yihua Zhang is also affiliated to Baioupai Tianjin Biotechnology Ltc., Tianjin, China.

## Acknowledgments

We thank the editors from American Journal Experts for editing the English text of a draft of this manuscript.

## Author Contributions

D.G. carried out the experiments, analyzed the data, and drafted the manuscript. Y.Z. designed the study, reviewed the data, and revised the manuscript. P.D., Z.F. and J.W. conducted parts of the experiments. All authors have read and agreed to the published version of the manuscript.

## Ethical Approval

Ethical Approval is not applicable for this article.

## Statement of Human and Animal Rights

This article does not contain any studies with human or animal subjects.

## Statement of Informed Consent

There are no human subjects in this article and informed consent is not applicable.

## Declaration of Conflicting Interests

The author(s) declared no potential conflicts of interest with respect to the research, authorship, and/or publication of this article.

## Funding

The author(s) disclosed receipt of the following financial support for the research, authorship, and/or publication of this article: This work was supported by the National Natural Science Foundation of China (project number: 31872529) and the Key Project of Natural Science Foundation of Shaanxi Province (project number: 2019JZ-16) in the design of study, data analysis, and writing of the manuscript.

## ORCID iDs

Dengke Gao  <https://orcid.org/0000-0001-9751-7214>

Yihua Zhang  <https://orcid.org/0000-0002-2939-5187>

## Supplemental Material

Supplemental material for this article is available online.

## References

1. Nelson RW, Reusch CE. Animal models of disease: classification and etiology of diabetes in dogs and cats. *J Endocrinol*. 2014;222(3):T1–9.
2. Rand JS, Fleeman LM, Farrow HA, Appleton DJ, Lederer R. Canine and feline diabetes mellitus: nature or nurture? *J Nutr*. 2004;134(Suppl 8): 2072s–80s.
3. Loke YK, Kwok CS, Singh S. Comparative cardiovascular effects of thiazolidinediones: systematic review and meta-analysis of observational studies. *BMJ*. 2011;342:d1309.
4. Stephenson J. Diabetes drug may be associated with increase in risk of bladder cancer. *JAMA*. 2011;306(2):143.
5. American Diabetes Association. 8. Pharmacologic approaches to glycemic treatment: standards of medical care in diabetes-2018. *Diabetes Care*. 2018;41(Suppl 1):S73–85.
6. Farney AC, Sutherland DE, Opara EC. Evolution of islet transplantation for the last 30 years. *Pancreas*. 2016;45(1):8–20.
7. Quiskamp N, Bruin JE, Kieffer TJ. Differentiation of human pluripotent stem cells into  $\beta$ -cells: potential and challenges. *Best Pract Res Clin Endocrinol Metab*. 2015;29(6):833–47.
8. Cierpka-Kmiec K, Wronska A, Kmiec Z. In vitro generation of pancreatic  $\beta$ -cells for diabetes treatment. I.  $\beta$ -like cells derived from human pluripotent stem cells. *Folia Histochem Cytobiol*. 2019;57(1):1–14.
9. Boháčová P, Holáň V. Mesenchymal stem cells and type 1 diabetes treatment. *Vnitr Lek*. 2018;64(7–8):725–28.
10. Páth G, Perakakis N, Mantzoros CS, Seufert J. Stem cells in the treatment of diabetes mellitus—focus on mesenchymal stem cells. *Metabolism*. 2019;90:1–15.

11. Limbert C, Páth G, Ebert R, Rothhammer V, Kassem M, Jakob F, Seufert J. PDX1- and NGN3-mediated in vitro reprogramming of human bone marrow-derived mesenchymal stromal cells into pancreatic endocrine lineages. *Cytotherapy*. 2011; 13(7):802–13.
12. Li HT, Jiang FX, Shi P, Zhang T, Liu XY, Lin XW, San ZY, Pang XN. In vitro reprogramming of rat bmMSCs into pancreatic endocrine-like cells. *In Vitro Cell Dev Biol Anim*. 2017; 53(2):157–66.
13. Solis MA, Moreno Velásquez I, Correa R, Huang LLH. Stem cells as a potential therapy for diabetes mellitus: a call-to-action in Latin America. *Diabetol Metab Syndr*. 2019;11:20.
14. Mafi R, Hindocha S, Mafi P, Griffin M, Khan WS. Sources of adult mesenchymal stem cells applicable for musculoskeletal applications—a systematic review of the literature. *Open Orthop J*. 2011;5(Suppl 2):242–48.
15. Gradwohl G, Dierich A, LeMeur M, Guillemot F. neurogenin3 is required for the development of the four endocrine cell lineages of the pancreas. *Proc Natl Acad Sci U S A*. 2000;97(4):1607–11.
16. Wang J, Elghazi L, Parker SE, Kizilocak H, Asano M, Sussel L, Sosa-Pineda B. The concerted activities of Pax4 and Nkx2.2 are essential to initiate pancreatic beta-cell differentiation. *Dev Biol*. 2004;266(1):178–89.
17. Wang YC, Gallego-Arteche E, Iezza G, Yuan XC, Matli MR, Choo SP, Zuraek MB, Gogia R, Lynn FC, German MS, Bergsland EK, et al. Homeodomain transcription factor NKX2.2 functions in immature cells to control enteroendocrine differentiation and is expressed in gastrointestinal neuroendocrine tumors. *Endocr Relat Cancer*. 2009;16(1):267–79.
18. Tabar MH, Tabandeh MR, Moghimipour E, Dayer D, Ghadiri AA, Bakhshi EA, Orazizadeh M, Ghafari MA. The combined effect of Pdx1 overexpression and Shh manipulation on the function of insulin-producing cells derived from adipose-tissue stem cells. *Febs Open Bio*. 2018;8(3):372–82.
19. Xu LF, Xu CJ, Zhou SP, Liu XK, Wang J, Liu XK, Qian SP, Xin YR, Gao Y, Zhu YQ, Tang XL. PAX4 promotes PDX1-induced differentiation of mesenchymal stem cells into insulin-secreting cells. *Am J Transl Res*. 2017;9(3):874–86.
20. Zhang T, Wang H, Wang T, Wei C, Jiang H, Jiang S, Yang J, Shao J, Ma L. Pax4 synergistically acts with Pdx1, Ngn3 and MafA to induce HuMSCs to differentiate into functional pancreatic  $\beta$ -cells. *Exp Ther Med*. 2019;18(4):2592–98.
21. Wei Y, Fang J, Cai S, Lv C, Zhang S, Hua J. Primordial germ cell-like cells derived from canine adipose mesenchymal stem cells. *Cell Prolif*. 2016;49(4):503–11.
22. Wang JL, Dai PX, Gao DK, Zhang X, Ruan CM, Li JK, Chen YJ, Zhang LW, Zhang YH. Genome-wide analysis reveals changes in long noncoding RNAs in the differentiation of canine BMSCs into insulin-producing cells. *Int J Mol Sci*. 2020;21(15):5549.
23. Livak KJ, Schmittgen TD. Analysis of relative gene expression data using real-time quantitative PCR and the 2(T)(-Delta C) method. *Methods*. 2001;25(4):402–408.
24. Zhao W, Zou T, Cui H, Lv YG, Gao DK, Ruan CM, Zhang X, Zhang YH. Parathyroid hormone (1-34) promotes the effects of 3D printed scaffold-seeded bone marrow mesenchymal stem cells on meniscus regeneration. *Stem Cell Res Ther*. 2020;11(1):328.
25. Zhang YH, Dou ZY. Under a nonadherent state, bone marrow mesenchymal stem cells can be efficiently induced into functional islet-like cell clusters to normalize hyperglycemia in mice: a control study. *Stem Cell Res Ther*. 2014;5:66.
26. Zhang YH, Shen WZ, Hua JL, Lei AM, Lv CR, Wang HY, Yang CR, Gao ZM, Dou ZY. Pancreatic islet-like clusters from bone marrow mesenchymal stem cells of human first-trimester abortus can cure streptozocin-induced mouse diabetes. *Rejuvenation Res*. 2010;13(6):695–706.
27. Lilly MA, Davis MF, Fabie JE, Terhune EB, Gallicano GI. Current stem cell based therapies in diabetes. *Am J Stem Cells*. 2016;5(3):87–98.
28. Antuna-Puente B, Feve B, Fellahi S, Bastard JP. Obesity, inflammation and insulin resistance: which role for adipokines? *Therapie*. 2007;62(4):285–92.
29. Kajiyama H, Hamazaki TS, Tokuhara M, Masui S, Okabayashi K, Ohnuma K, Yabe S, Yasuda K, Ishiura S, Okochi H, Asashima M. Pdx1-transfected adipose tissue-derived stem cells differentiate into insulin-producing cells in vivo and reduce hyperglycemia in diabetic mice. *Int J Dev Biol*. 2010; 54(4):699–705.
30. Bahrebar M, Soleimani M, Karimi MH, Vahdati A, Yaghobi R. Generation of islet-like cell aggregates from human adipose tissue-derived stem cells by lentiviral overexpression of PDX-1. *Int J Organ Transplant Med*. 2015;6(2):61–76.
31. Deng W, Yang D, Zhao B, Ouyang Z, Song J, Fan N, Liu Z, Zhao Y, Wu Q, Nashun B, Tang J, et al. Use of the 2A peptide for generation of multi-transgenic pigs through a single round of nuclear transfer. *PLoS ONE*. 2011;6(5):e19986.
32. Brokhman I, Pomp O, Fishman L, Tennenbaum T, Amit M, Itzkovitz-Eldor J, Goldstein RS. Genetic modification of human embryonic stem cells with adenoviral vectors: differences of infectability between lines and correlation of infectability with expression of the coxsackie and adenovirus receptor. *Stem Cells Dev*. 2009;18(3):447–56.
33. Chinnasamy D, Milsom MD, Shaffer J, Neuenfeldt J, Shaaban AF, Margison GP, Fairbairn LJ, Chinnasamy N. Multicistronic lentiviral vectors containing the FMDV 2A cleavage factor demonstrate robust expression of encoded genes at limiting MOI. *Virology*. 2006;3:14.
34. Kim JH, Lee SR, Li LH, Park HJ, Park JH, Lee KY, Kim MK, Shin BA, Choi SY. High cleavage efficiency of a 2A peptide derived from porcine teschovirus-1 in human cell lines, zebrafish and mice. *PLoS ONE*. 2011;6(4):e18556.
35. Gao R, Ustinov J, Pulkkinen MA, Lundin K, Korsgren O, Otonkoski T. Characterization of endocrine progenitor cells and critical factors for their differentiation in human adult pancreatic cell culture. *Diabetes*. 2003;52(8):2007–15.
36. Xu H, Tsang KS, Chan JC, Yuan P, Fan R, Kaneto H, Xu G. The combined expression of Pdx1 and MafA with either Ngn3 or NeuroD improves the differentiation efficiency of mouse embryonic stem cells into insulin-producing cells. *Cell Transplant*. 2013;22(1):147–58.
37. Kubo A, Stull R, Takeuchi M, Bonham K, Gouon-Evans V, Sho M, Iwano M, Saito Y, Keller G, Snodgrass R. Pdx1 and Ngn3 overexpression enhances pancreatic differentiation of mouse ES cell-derived endoderm population. *PLoS ONE*. 2011;6(9):e24058.
38. Sommer CA, Stadtfeld M, Murphy GJ, Hochedlinger K, Kotton DN, Mostoslavsky G. Induced pluripotent stem cell generation using a single lentiviral stem cell cassette. *Stem Cells*. 2009;27(3):543–49.